ChemPubSoc Europe

DOI: 10.1002/cctc.201700809

CHEMCATCHEM Communications

Plasma-Assisted Synthesis of Monodispersed and Robust Ruthenium Ultrafine Nanocatalysts for Organosilane Oxidation and Oxygen Evolution Reactions

Edwin S. Gnanakumar,[a] Wesley Ng,[a] Bilge Coşkuner Filiz,[a] Gadi Rothenberg,[a] Sheng Wang,[b] Hualong Xu,[b] Laura Pastor-Pérez,[c] M. Mercedes Pastor-Blas,[c] Antonio Sepúlveda-Escribano,[c] Ning Yan,*[a] and N. Raveendran Shiju*[a]

We report a facile and general approach for preparing ultrafine ruthenium nanocatalysts by using a plasma-assisted synthesis at $<100\,^{\circ}C$. The resulting Ru nanoparticles are monodispersed (typical size 2 nm) and remain that way upon loading onto carbon and TiO_2 supports. This gives robust catalysts with excellent activities in both organosilane oxidation and the oxygen evolution reaction.

Heterogeneous catalysts often consist of small metal particles dispersed on supports.[1–4] Although many methods have been proposed for their synthesis,[5–7] the most common approach involves impregnating the support with a metal precursor solution, followed by thermal decomposition and reduction at a relatively high temperature.[8–10] The problem is that these steps often cause sintering and/or agglomeration.[2–4,11] Moreover, many "too-small-to-be-stable" nanoparticles form through the Ostwald ripening mechanism.[12] The result is a broad particle-size distribution, which lowers catalyst performance.[10,13–15] Alternatively, one can use strong reducing agents, such as sodium borohydride and hydrazine, to convert the precursors into the corresponding metals, but many of these reductants are corrosive and/or toxic and can cause further problems downstream.[16,17] Hence, most of today's syntheses of monodispersed nanocrystals are based on colloidal chemical synthetic procedures involving the use of capping agents and spacers, which hamper large-scale applications.

[a] Dr. E. S. Gnanakumar, W. Ng, Dr. B. Coşkuner Filiz, Prof. Dr. G. Rothenberg, Dr. N. Yan, Dr. N. R. Shiju
Van't Hoff Institute for Molecular Sciences
University of Amsterdam
P.O. Box 94157, 1090GD Amsterdam (The Netherlands)
E-mail: n.yan@uva.nl
n.r.shiju@uva.nl

[b] S. Wang, Prof. Dr. H. Xu
Shanghai Key Lab of Molecular Catalysis and Innovative Materials, Department of Chemistry
Fudan University
Shanghai 200433 (P.R. China)

[c] L. Pastor-Pérez, Prof. Dr. M. M. Pastor-Blas, Prof. Dr. A. Sepúlveda-Escribano
Departamento de Química Inorgánica,
Instituto Universitario de Materiales de Alicante
Universidad de Alicante
Ap. 99, E-03080 Alicante (Spain)

Supporting Information for this article can be found under: https://doi.org/10.1002/cctc.201700809.

One way to avoid these problems is by using plasma-assisted synthesis.[18,19] This method produces nanoparticles and metal-supported catalysts from metal precursors.[18,20,21] Some of the supported catalysts prepared by the plasma-assisted synthesis method are Au/Y-zeolite,[22] Pt/Y-zeolite,[22] Pt/γ-Al_2O_3,[23] Co/γ-Al_2O_3,[23] Ni/γ-Al_2O_3,[24] Pt/Al_2O_3-CeO_2,[25] Co/C,[26] and Fe/C.[26] This method is simple, quick, and compatible with impregnation processes.[27] However, these thermal plasma techniques do not always give good control of the particle size.[28] In these processes, the nanoparticles undergo rapid agglomeration because of the high temperatures, which may result in broad particle-size distributions.[28]

Herein, we report a cold plasma-assisted approach for the preparation of supported ruthenium catalysts.[27–30] This method has excellent support compatibility (we used carbon as well as titania supports), which enables the synthesis of monodispersed and ultrafine Ru nanoparticles. Cold plasma synthesis is solvent-free and ligand-free, giving high-purity nanoparticles. We tested these catalysts in two representative yet different reactions: organosilane oxidation and the oxygen evolution reaction (OER). Previous organosilane oxidations were performed mainly by using metals such as gold,[31–36] palladium,[8,32] platinum,[37] and rhodium.[38] The costs of these metals are 38, 24, 31, and 285 $\$\,g^{-1}$, respectively (January 2017).[39] Although ruthenium is much cheaper (1.3 $\$\,OZT^{-1}$), it has rarely been used for silane oxidation. The OER is the rate-determining step in many important energy-related processes such as water splitting, reversible metal–air batteries, and fuel cells.[40,41] Ruthenium oxide (RuO_2) is one of the best-performing OER catalysts to date.[42–44] Thus, we decided to focus on Ru catalysts, and in both reactions the catalysts showed high activity and stability.

Figure 1 illustrates the facile preparation procedures for the carbon-supported 5 wt% Ru catalyst (denoted hereafter as Ru-Plasma) by a cold plasma synthesis (detailed experimental procedures are included in the Supporting Information). The low-temperature process ($<100\,^{\circ}C$) gave ultrafine and monodispersed Ru nanoparticles on the support. Conversely, conventional calcination requires at least $400\,^{\circ}C$ to decompose the $RuCl_3$ precursor (see the coupled thermogravimetric and differential scanning calorimetric analyses in Figure S2 in the Supporting Information). Combined with sequential reduction in H_2, it causes the agglomeration of the Ru nanoparticles.

The powder X-ray diffraction (XRD) pattern of Ru-Plasma in Figure 2a confirms the complete decomposition of $RuCl_3$ and

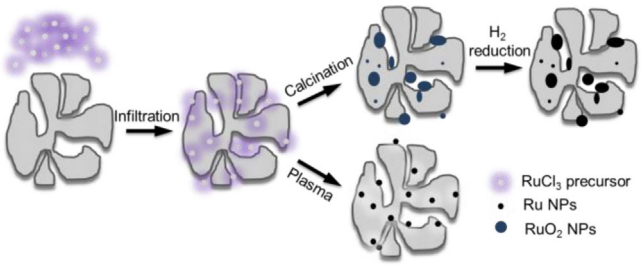

Figure 1. A comparison of the workflows for the preparation of supported Ru catalysts by conventional calcination–reduction and plasma-assisted synthesis.

the formation of metallic Ru after plasma treatment. By comparing with the pattern of commercial 5 wt% Ru on carbon (denoted hereafter as Ru-Conv), we attribute the broad peaks at $2\theta = 24.0$ and 43.5° to carbon (graphite) and the tiny peaks from $2\theta = 38.4$ to 44° to metallic Ru.[45] X-ray photoelectron spectroscopy (XPS) also reveals the effectiveness of the plasma synthesis. Indeed, overlapping of the C 1s and Ru 3d core levels poses a challenge upon analyzing the spectrum in Figure 2b, particularly at low Ru loadings. Nonetheless, there is a clear binding-energy shift in the Ru $3d_{5/2}$ peak relative to its position in the sample before plasma treatment, which implies a decrease in the Ru oxidation state (see inset).[46,47] We also studied the crystal structure of Ru-Plasma through high- resolution transmission electron microscopy (HRTEM). Figure 2c shows the atom-resolved micrographs of two Ru compound particles; the 2.3 Å *d* spacing indicates the (1 0 0) plane of metallic Ru crystal.[48,49]

Thanks to the plasma treatment, Ru-Plasma has a highly uniform particle-size distribution. Figure 2d,e shows that nearly all of the Ru nanoparticles have dimensions between 1 and 2 nm. In contrast, the Ru particle-size distribution in commercial Ru-Conv is much wider (see Figure 2f,g). There are many too-small (< 1 nm, blue arrow) and too-large (> 5 nm, yellow arrow) Ru nanoparticles that reduce performance (more TEM results of Ru-Plasma are included in the Supporting Information). This confirms the hypothesis of sintering by Ostwald ripening: the small particles become even smaller as the big ones grow bigger, a "big-fish-eat-small-fish" effect.[12] In addition, Ru-Plasma has a higher specific surface area (1298 $m^2 g^{-1}$) than Ru-Conv (713 $m^2 g^{-1}$) according to standard N_2 adsorption measurements, due to its finer nanostructure.

Ru-Plasma showed excellent activity and stability in a number of chemical and electrochemical reactions. We initially performed organosilane oxidation to organosilanol by using water as an oxidant under ambient conditions (see Scheme 1 and Table 1). Our catalyst produced organosilanols selectively. H_2 gas was the sole byproduct, and no disiloxanes were observed, unlike conventional approaches.[31–38,50–53] The reported reactions were conducted at high temperature and/or under an O_2 atmosphere, and the turnover number (TON) was not usually higher than 20.[32,36] With dimethylphenylsilane as the model substrate, our Ru-Plasma catalyst showed a turnover frequency (TOF) of 29 min^{-1} at room temperature. Conversely, Ru-Conv showed a TOF of only 6 min^{-1} (see Table 1, entry 4), which reflects the presence of less-active sites. At 40 °C, the TOF increased to 44 min^{-1} with the Ru-Plasma catalyst, even though we doubled the silane/Ru molar ratio to 2637 (Table 1,

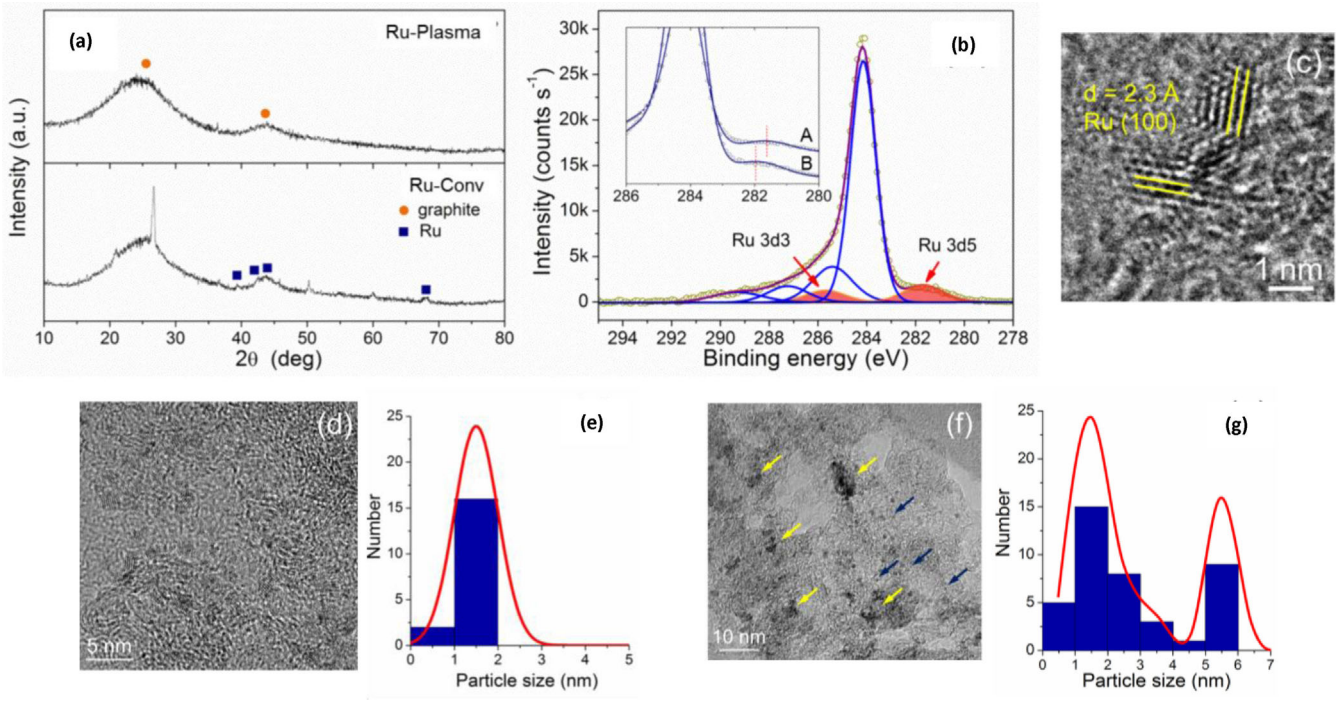

Figure 2. a) XRD patterns of Ru-Plasma and Ru-Conv. b) Deconvoluted X-ray photoelectron spectra of the C 1s and Ru 3d core levels. A and B in the inset compare the fitted envelopes in the region of Ru $3d^5$ for Ru-Plasma before and after plasma treatment. c) HRTEM micrograph of Ru nanoparticles on carbon. TEM images of the d) Ru-Plasma and f) Ru-Conv catalysts and e,g) the corresponding particle-size distribution plots.

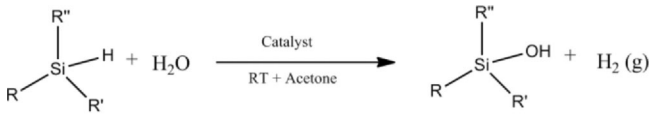

1a R, R'=CH_3, R"=C_6H_5 **1d** R=H, R'=CH_3, R"-C_6H_5

1b R, R', R"=C_6H_5 **1e** R,R',R"=C_2H_5

1c R, R'=C_6H_5, R"=CH_3 **1f** R=H, R',R"=C_6H_5

Scheme 1. Oxidation of organosilane to silanol with water by using supported Ru catalysts.

Table 1. Organosilane oxidation to silanol by using supported Ru catalysts.[a]

Entry	Catalyst	Substrate	Conv. [%]	*T* [min]	TON	TOF [min^{-1}]
1	Ru-Plasma	Me_2PhSiH (**1a**)	>99	45	1318	29
2	Ru-Plasma	Me_2PhSiH (**1a**)	>99[b]	60	2637	44
3	Ru-Plasma	Me_2PhSiH (**1a**)	>99[b]	140	5274	38
4	Ru-Conv	Me_2PhSiH (**1a**)	>99	210	1318	6
5	Ru-Plasma	Ph_3SiH (**1b**)	>99	30	500	17
6	Ru-Plasma	$MePh_2SiH$ (**1c**)	>99	50	500	10
7	Ru-Plasma	$PhMeSiH_2$ (**1d**)	>99	25	500	20
8	Ru-Plasma	Et_3SiH (**1e**)	>99	20	500	25
9	Ru-Plasma	Ph_2SiH_2 (**1f**)	>99	35	500	14.3
10	none	Me_2PhSiH (**1a**)	0	180	100	0

[a] Reaction conditions: catalyst (25 mg), H_2O (2 mL, as oxidant), acetone (5 mL), 25 °C. [b] Reaction was performed at 40 °C.

entry 2). The reaction proceeded to complete conversion even at a higher silane/Ru ratio of 5274 with a TOF of 37.7 min^{-1} (Table 1, entry 3).

Ru-Plasma was also active for the oxidation of other organosilanes (Table 1, entries 5–9). Control experiments confirmed that no reaction took place in the absence of the catalyst or only with the carbon support. The selectivity to silanol was >99%. No disiloxane was detected, ruling out silanol condensation. Interestingly, the spent Ru-Plasma catalyst retained high activity and selectivity after three consecutive runs, indicating its stability (see the TEM image of the spent catalyst in the Supporting Information). We then prepared titania-supported Ru catalysts by the same synthesis route. These also had monodispersed Ru nanoparticles and showed excellent activity in organosilane oxidation reactions (see the Supporting Information for details), which suggests good support compatibility of the new synthesis approach.

A new catalyst synthesis protocol is much more useful if it can be applied to different reaction scenarios. We therefore examined the performance of the Ru-Plasma catalyst in the electrochemical oxygen evolution reaction. However, the "too-small" Ru nanoparticles corroded if the OER potential was applied (RuO_4^{2-} was soluble in the reaction medium).[42,54] Thus, careful control of the nanostructure of the catalyst is important. Figure S6 shows the cyclic voltammetry (CV) curve of Ru-Plasma in 0.05 M deoxygenated H_2SO_4. The redox peaks were attributed to the hydrolysis of Ru [Eq. (1)],[55] in agreement with the formation of metallic Ru after plasma treatment.

$$Ru + H_2O \leftrightarrow RuOH + H^+ + e^- \quad (1)$$

Figure 3 shows the 20 cycle CV curves of Ru-Plasma and Ru-Conv in oxygen-saturated electrolyte from 0.8 to 1.58 V versus the reversible hydrogen electrode (RHE) (overpotential, η = 0.3 V). Apparently, Ru-Conv suffered instant oxidation at approximately 1.51 V versus RHE in the first cycle (see the anodic

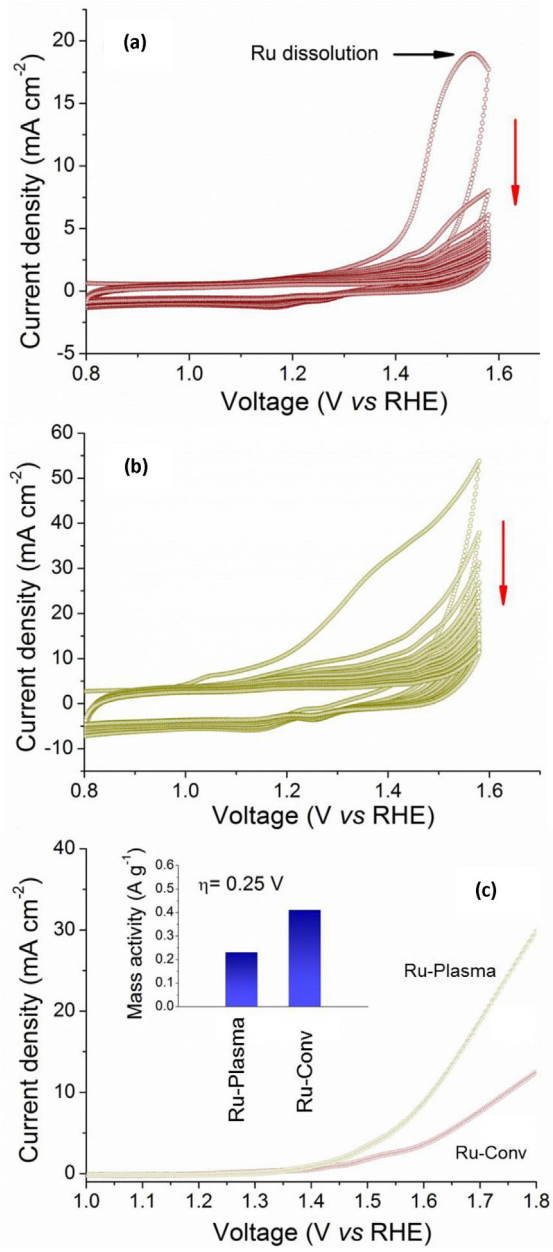

Figure 3. 20 cycle CV plots of the a) Ru-Conv and b) Ru-Plasma catalysts in O_2-saturated 0.05 M H_2SO_4 from 0.8 to 1.58 V vs. RHE. c) A comparison of the OER LSV curves for the Ru-Conv and Ru-Plasma catalysts after CV cycling. The scan rate was 10 mV s^{-1}, the rotating speed of the rotating disc electrode was 1600 rpm, and *iR* correction was applied; the inset shows the mass activity of both catalysts at η = 0.25 V.

peak indicated by the arrow), which has been widely documented as the sequence of Ru-nanoparticle dissolution.[42,54] A large portion of Ru nanoparticles in Ru-Conv was less than 1 nm in size (see Figure 2) and was inherently more susceptible to deep oxidation to form soluble RuO_4^{2-} species.[42,54] Conversely, this was not observed on Ru-Plasma; gradual current degradation was owing to the accumulation of oxygen bubbles that blocked the working electrode. We then ran linear sweep voltammetry (LSV) while rotating the electrode at a scan rate of 10 mV s^{-1} to study the OER activity as well as the stability of both catalysts (see Figure 3c). The OER onset potentials were essentially identical for both catalysts, as RuO_2 itself is an excellent OER catalyst. At $\eta = 0.25$ V, the mass activity of Ru-Plasma reached 0.41 A g^{-1}, which was nearly double that of Ru-Conv and better than that of most 5 wt% Ru catalysts previously reported.[43] Though oxygen bubbles were removed, the Ru-Conv catalyst showed more significant performance loss than the Ru-Plasma catalyst. These observations reflect the good structural stability of Ru-Plasma, which can sustain more Ru nanoparticles (active sites) than Ru-Conv after applying OER potentials. A broad peak at approximately 1.54 V in the LSV curve of the Ru-Conv sample might be related to the oxidation of Ru nanoparticles. We also performed several cycles of LSV for the Ru-Plasma catalyst, which showed reproducibility and thus stability (see the Supporting Information).

In summary, our results show that plasma treatment effectively decomposes $RuCl_3$ to Ru nanoparticles under near-ambient conditions. The resulting metal particles on both carbon and TiO_2 supports were ultrafine and monodispersed. In particular, the Ru-Plasma catalyst demonstrated significantly higher activity and stability in both organosilane oxidation and the oxygen evolution reaction than the catalyst made by the conventional method. As we showed, the method could be applied successfully for multiple supports, indicating its general use.

Acknowledgements

N.R.S. and E.S.G. acknowledge financial support from the NWO CAPITA project (732.013.002). A.S.E. acknowledges financial support from Generalitat Valenciana, Spain (Project PROMETEOII/2014/004). This work is part of the Research Priority Area Sustainable Chemistry of the University of Amsterdam, http://suschem.uva.nl

Keywords: nanostructures · oxidation · plasma chemistry · ruthenium · supported catalysts

[1] M. Campanati, G. Fornasari, A. Vaccari, *Catal. Today* **2003**, *77*, 299 – 314.
[2] F. Pinna, *Catal. Today* **1998**, *41*, 129 – 137.
[3] C. Perego, P. Villa, *Catal. Today* **1997**, *34*, 281 – 305.
[4] N. Yan, J. Pandey, Y. M. Zeng, B. S. Amirkhiz, B. Hua, N. J. Geels, J. L. Luo, G. Rothenberg, *ACS Catal.* **2016**, *6*, 4630 – 4634.
[5] J. Lu, J. W. Elam, P. C. Stair, *Acc. Chem. Res.* **2013**, *46*, 1806 – 1815.
[6] N. Herron, W. E. Farneth, *Adv. Mater.* **1996**, *8*, 959 – 968.
[7] K. L. Fujdala, T. D. Tilley, *J. Catal.* **2003**, *216*, 265 – 275.
[8] K. Mori, K. Yamaguchi, T. Hara, T. Mizugaki, K. Ebitani, K. Kaneda, *J. Am. Chem. Soc.* **2002**, *124*, 11572 – 11573.
[9] A. T. Bell, *Science* **2003**, *299*, 1688 – 1691.
[10] P. Demma Carà, M. Pagliaro, A. Elmekawy, D. R. Brown, P. Verschuren, N. R. Shiju, G. Rothenberg, *Catal. Sci. Technol.* **2013**, *3*, 2057 – 2061.
[11] S. Tauster, S. Fung, R. Garten, *J. Am. Chem. Soc.* **1978**, *100*, 170 – 175.
[12] T. W. Hansen, A. T. Delariva, S. R. Challa, A. K. Datye, *Acc. Chem. Res.* **2013**, *46*, 1720 – 1730.
[13] S.-W. Ho, J. M. Cruz, M. Houalla, D. M. Hercules, *J. Catal.* **1992**, *135*, 173 – 185.
[14] Y. Brik, M. Kacimi, M. Ziyad, F. Bozon-Verduraz, *J. Catal.* **2001**, *202*, 118 – 128.
[15] C. Hernandez-Mejia, E. S. Gnanakumar, A. Olivos-Suarez, J. Gascon, H. F. Greer, W. Zhou, G. Rothenberg, N. R. Shiju, *Catal. Sci. Technol.* **2016**, *6*, 577 – 582.
[16] K. P. de Jong, *Synthesis of solid catalysts*, Wiley-VCH, Weinheim, **2009**.
[17] J.-J. Zou, Y.-p. Zhang, C.-J. Liu, *Langmuir* **2006**, *22*, 11388 – 11394.
[18] C.-j. Liu, G. P. Vissokov, B. W.-L. Jang, *Catal. Today* **2002**, *72*, 173 – 184.
[19] W. Chu, J. Q. Xu, J. P. Hong, T. Lin, A. Khodakov, *Catal. Today* **2015**, *256*, 41 – 48.
[20] P. A. Lin, R. M. Sankaran, *Angew. Chem. Int. Ed.* **2011**, *50*, 10953 – 10956; *Angew. Chem.* **2011**, *123*, 11145 – 11148.
[21] J. Zheng, R. Yang, L. Xie, J. L. Qu, Y. Liu, X. G. Li, *Adv. Mater.* **2010**, *22*, 1451 – 1473.
[22] J. C. Legrand, A. M. Diamy, G. Riahi, Z. Randriamanantenasoa, M. Polisset-Thfoin, J. Fraissard, *Catal. Today* **2004**, *89*, 177 – 182.
[23] S. S. Kim, H. Lee, B. K. Na, H. K. Song, *Catal. Today* **2004**, *89*, 193 – 200.
[24] X. L. Zhu, P. P. Huo, Y. P. Zhang, D. G. Cheng, C. J. Liu, *Appl. Catal. B* **2008**, *81*, 132 – 140.
[25] F. Rahmani, M. Haghighi, P. Estifaee, *Microporous Mesoporous Mater.* **2014**, *185*, 213 – 223.
[26] J. Aluha, P. Boahene, A. Dalai, Y. F. Hu, K. Bere, N. Braidy, N. Abatzoglou, *Ind. Eng. Chem. Res.* **2015**, *54*, 10661 – 10674.
[27] R. Buitrago-Sierra, M. J. Garcia-Fernandez, M. M. Pastor-Blas, A. Sepulveda-Escribano, *Green Chem.* **2013**, *15*, 1981 – 1990.
[28] U. R. Kortshagen, R. M. Sankaran, R. N. Pereira, S. L. Girshick, J. J. Wu, E. S. Aydil, *Chem. Rev.* **2016**, *116*, 11061 – 11127.
[29] M. Rivallan, I. Yordanov, S. Thomas, C. Lancelot, S. Mintova, F. Thibault-Starzyk, *ChemCatChem* **2010**, *2*, 1074 – 1078.
[30] T. Witvrouwen, S. Paulussen, B. Sels, *Plasma Processes Polym.* **2012**, *9*, 750 – 760.
[31] T. Mitsudome, A. Noujima, T. Mizugaki, K. Jitsukawa, K. Kaneda, *Chem. Commun.* **2009**, 5302 – 5304.
[32] M. Jeon, J. Han, J. Park, *ChemCatChem* **2012**, *4*, 521 – 524.
[33] V. Gitis, R. Beerthuis, N. R. Shiju, G. Rothenberg, *Catal. Sci. Technol.* **2014**, *4*, 2156 – 2160.
[34] N. Asao, Y. Ishikawa, N. Hatakeyama, Menggenbateer, Y. Yamamoto, M. Chen, W. Zhang, A. Inoue, *Angew. Chem. Int. Ed.* **2010**, *49*, 10093 – 10095; *Angew. Chem.* **2010**, *122*, 10291 – 10293.
[35] J. John, E. Gravel, A. Hagege, H. Li, T. Gacoin, E. Doris, *Angew. Chem. Int. Ed.* **2011**, *50*, 7533 – 7536; *Angew. Chem.* **2011**, *123*, 7675 – 7678.
[36] K. Mori, M. Tano, T. Mizugaki, K. Ebitani, K. Kaneda, *New J. Chem.* **2002**, *26*, 1536 – 1538.
[37] B. P. S. Chauhan, A. Sarkar, M. Chauhan, A. Roka, *Appl. Organomet. Chem.* **2009**, *23*, 385 – 390.
[38] M. Yu, H. Jing, X. Fu, *Inorg. Chem.* **2013**, *52*, 10741 – 10743.
[39] http://www.infomine.com/investment/metal-prices/ruthenium/.
[40] F. Y. Cheng, J. Chen, *Chem. Soc. Rev.* **2012**, *41*, 2172 – 2192.
[41] M. G. Walter, E. L. Warren, J. R. McKone, S. W. Boettcher, Q. X. Mi, E. A. Santori, N. S. Lewis, *Chem. Rev.* **2010**, *110*, 6446 – 6473.
[42] T. Reier, M. Oezaslan, P. Strasser, *ACS Catal.* **2012**, *2*, 1765 – 1772.
[43] E. A. Paoli, F. Masini, R. Frydendal, D. Deiana, C. Schlaup, M. Malizia, T. W. Hansen, S. Horch, I. E. L. Stephens, I. Chorkendorff, *Chem. Sci.* **2015**, *6*, 190 – 196.
[44] V. Petrykin, K. Macounova, O. A. Shlyakhtin, P. Krtil, *Angew. Chem. Int. Ed.* **2010**, *49*, 4813 – 4815; *Angew. Chem.* **2010**, *122*, 4923 – 4925.
[45] S. Iqbal, S. A. Kondrat, D. R. Jones, D. C. Schoenmakers, J. K. Edwards, L. Lu, B. R. Yeo, P. P. Wells, E. K. Gibson, D. J. Morgan, *ACS Catal.* **2015**, *5*, 5047 – 5059.
[46] K. Kim, N. Winograd, *J. Catal.* **1974**, *35*, 66 – 72.
[47] K. Qadir, S. H. Joo, B. S. Mun, D. R. Butcher, J. R. Renzas, F. Aksoy, Z. Liu, G. A. Somorjai, J. Y. Park, *Nano Lett.* **2012**, *12*, 5761 – 5768.

[48] V. Jain, R. Sahoo, J. R. Jinschek, R. Montazami, H. M. Yochum, F. L. Beyer, A. Kumar, J. R. Heflin, *Chem. Commun.* **2008**, 3663 – 3665.
[49] K. Guo, Y. Li, J. Yang, Z. Zou, X. Xue, X. Li, H. Yang, *J. Mater. Chem. A* **2014**, *2*, 1509 – 1514.
[50] A. K. L. Teo, W. Y. Fan, *Chem. Commun.* **2014**, *50*, 7191 – 7194.
[51] T. Mitsudome, S. Arita, H. Mori, T. Mizugaki, K. Jitsukawa, K. Kaneda, *Angew. Chem. Int. Ed.* **2008**, *47*, 7938 – 7940; *Angew. Chem.* **2008**, *120*, 8056 – 8058.
[52] E. Choi, C. Lee, Y. Na, S. Chang, *Org. Lett.* **2002**, *4*, 2369 – 2371.
[53] E. A. Ison, R. A. Corbin, M. M. Abu-Omar, *J. Am. Chem. Soc.* **2005**, *127*, 11938 – 11939.
[54] E. A. Paoli, F. Masini, R. Frydendal, D. Deiana, P. Malacrida, T. W. Hansen, I. Chorkendorff, I. E. L. Stephens, *Catal. Today* **2016**, *262*, 57 – 64.
[55] M. B. Vukmirovic, R. L. Sabatini, R. R. Adzic, *Surf. Sci.* **2004**, *572*, 269 – 276.

Manuscript received: May 16, 2017
Revised manuscript received: July 17, 2017
Accepted manuscript online: July 17, 2017
Version of record online: ■■ ▮▮, 0000

COMMUNICATIONS

E. S. Gnanakumar, W. Ng,
B. Coşkuner Filiz, G. Rothenberg, S. Wang,
H. Xu, L. Pastor-Pérez, M. M. Pastor-Blas,
*A. Sepúlveda-Escribano, N. Yan,**
*N. R. Shiju**

■■ – ■■

Plasma-Assisted Synthesis of Monodispersed and Robust Ruthenium Ultrafine Nanocatalysts for Organosilane Oxidation and Oxygen Evolution Reactions

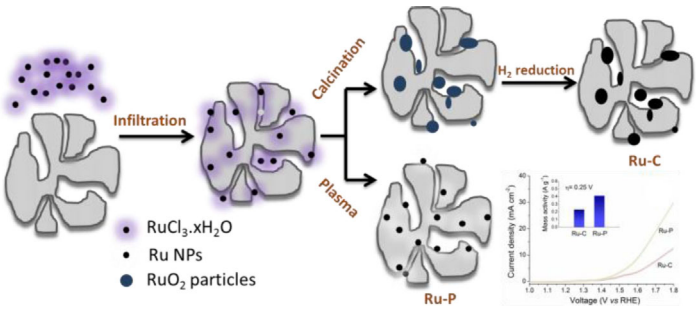

Out in the cold: Supported ruthenium catalysts prepared by a novel cold plasma-assisted approach show excellent activity in two representative yet different reactions: organosilane oxidation and oxygen evolution.

Heterogeneous & Homogeneous & Bio- & Nano-
CHEMCATCHEM
CATALYSIS

Supporting Information

Plasma-Assisted Synthesis of Monodispersed and Robust Ruthenium Ultrafine Nanocatalysts for Organosilane Oxidation and Oxygen Evolution Reactions

Edwin S. Gnanakumar,[a] Wesley Ng,[a] Bilge Coşkuner Filiz,[a] Gadi Rothenberg,[a] Sheng Wang,[b] Hualong Xu,[b] Laura Pastor-Pérez,[c] M. Mercedes Pastor-Blas,[c] Antonio Sepúlveda-Escribano,[c] Ning Yan,*[a] and N. Raveendran Shiju*[a]

cctc_201700809_sm_miscellaneous_information.pdf

1. Experimental section

1.1. Materials and instrumentation

The metal precursor, $RuCl_3$, was supplied by Sigma-Aldrich. The activated carbon support was RGC30 by MeadWestvaco, and the titania support was Degussa P25. Powder X-ray diffraction spectra were recorded using a Miniflex II diffractometer with Ni-filtered Cu Kα (λ=1.5406 Å) radiation. The X-ray tube was operated at 30 kV and 15 mA.[1] Surface area of the samples was determined by applying the BET method to the N_2 adsorption isotherms at -196 °C.[2] X-Ray photoelectron spectroscopy (XPS) was performed with a K-ALPHA spectrometer (Thermo Scientific). All spectra were collected using Al-Kα radiation (1486.6 eV), monochromatized by a twin crystal monochromator, yielding a focused X-ray spot with a diameter of 400 µm, at 3 mA × 12 kV. The alpha hemispherical analyser was operated at the constant energy mode with survey scan pass energies of 200 eV to measure the whole energy band and 50 eV in a narrow scan to selectively measure the particular elements. Charge compensation was achieved with the system flood gun that provides low energy electrons and low energy argon ions from a single source. The powder samples were pressed and mounted on the sample holder and placed in the vacuum chamber. Before recording the spectrum, the samples were maintained in the analysis chamber until a residual pressure of ca. 5×10^{-7} N m^{-2} was reached. The quantitative analysis was done by calculating the integral of each peak, after subtracting the S-shaped background, and by fitting the experimental curve to a combination of Lorentzian (30%) and Gaussian (70%) lines. Transmission electron microscopy (TEM) images were taken with a JEOL 2100 microscope (Japan) operated at 200 kV. Samples were firstly dispersed in ethanol and then dropped onto holey carbon films supported on Cu grids. The product analysis was carried out using a GC (Agilent model 7820A GC system, FID detector, ValcoBond VB capillary column with 30 m length, and 3 µm diameter).

1.2. Procedures for catalyst preparation

Supported ruthenium catalysts (Table 1) were prepared using either activated carbon or TiO_2 as supports. The supports were impregnated with an excess of aqueous solution of $RuCl_3 \cdot xH_2O$ (38.0-42.0 Ru basis, Aldrich, 10 ml solution/g of support) to obtain a 5 wt.% Ru loading. Excess of solvent was gently removed under vacuum in a rotary evaporator, and the solid was dried in an oven.

Each sample was loaded on an aluminium boat, which was placed in the glow discharge stainless steel cylindrical chamber of a Tucano plasma system (Gambetti Kenologia, Italy), provided with an anodized aluminium door. The HF electrode is made of aluminium, and it has a "Dark Shield", a RF 13.56 MHz power supply and mass flow controllers (MFC) for gas inlet control.[3] The reaction chamber was evacuated to mild vacuum (0.15 Torr) using a Pfeiffer rotary vacuum pump model PK D41 029C-Duo 2.5 with F4 Fomblin lubricant YL VAC 25/6. Then, argon was introduced into the plasma chamber over the specimen. Care was taken to pump down and purge the plasma reactor for at least 10 min prior to activating the RF field. The discharge power was set to 200 watts and 12 cycles of 5 min each were applied to each sample, with manual mixing of the sample between treatments to assure an even exposure to the plasma. The temperature of the sample after the plasma treatment was measured by non-contact infrared thermometer (PCE Instruments, model PCE-888). It could be determined that

the surface temperature was below 373 K in all cases. A schematic diagram of the plasma setup is shown in Figure 1.

1.3. Procedure for organosilane oxidation

The organosilane oxidation reaction was performed at room temperature (25°C) and atmospheric pressure. In this reaction, water was used as the oxidant and acetone was used as a solvent to homogenise the mixture. Thus, 0.38mL of dimethylphenylsilane was added to 0.5 mL of water and 5 ml of acetone in a 25 mL round bottom flask and a clear solution was obtained.[4] 10 mg of catalyst was then added (silane/Ru molar ratio=500). This oxidation reaction gave exclusively organosilanol as product, and no siloxanes were formed.

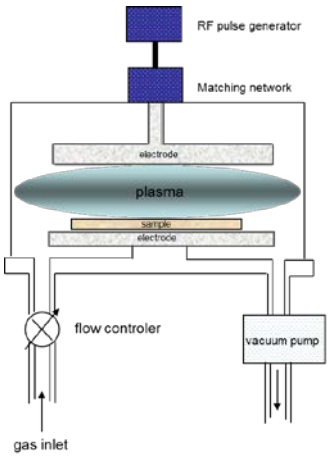

Figure S1. Schematic diagram of the RF-plasma treatment setup.

1.3. Procedure for electrochemical test

The performances of both commercial and plasma-synthesized 5 wt% ruthenium on carbon catalysts were evaluated in oxygen evolution reaction (OER). The catalyst inks were prepared according to the following recipe: 1 mL ethanol, 10 µL Nafion® (D-521 dispersion 5%wt in water/isopropanol, Alfa Aesar 42117) and 1 mg powder. The inks were sonicated overnight before being deposited to the glassy carbon electrode (Gamry, USA). The area of this circular working electrode was 0.196 cm^2, which was polished by diamond polishing films and rinsed well. Inks were deposited by dropcasting 5 µL per droplet x 6, with air drying between the drops. The total catalyst loading was 30 µg, or 153 µg/cm^2.

Electrochemical experiments were performed in a classic 3-electrode setup. A Gamry Reference 600 potentiostat was employed, together with a Gamry RDE710 Rotating Electrode setup. Saturated calomel electrode (SEC) and a graphite rod were used as the reference and counter electrode, respectively (Gamry, USA). 0.05 M H_2SO_4 was used as the electrolyte which was stabilized at 25.0 ± 0.1 °C in a water bath. We have tested Ir catalyst as an internal reference, we therefore used H_2SO_4 instead of $HClO_4$ that can be reduced by Ir at lower potential (~ 1 V). Potentials were reported vs. reversible hydrogen electrode (RHE) by adding 0.2991 for pH = 1.

Nitrogen (99.999%) or oxygen (99.999%) was bubbled for 30 minutes to saturate the solution. Cyclic voltammetry and linear scan voltammograms were measured at a scan rate of 100 mV/s and 10 mV/s, respectively. iR drop correction was applied in voltammetric measurements (typical resistance was between 30 to 50 Ω). Electrochemical impedance spectroscopy was performed potentiostatically at the OER over potential (η) of 0.25 V of (1.48V vs RHE). The impedance frequency range was 0.2 Hz to 106 Hz with an AC perturbation of 10 mV.

Table S1. Description of Ru-supported catalysts

No	Catalyst	Method of synthesis	Surface area of the catalyst in reduced state (m^2/g)
1	5Ru-Plasma	Plasma treated	1298
2	5Ru/Conv	Conventional synthesis	713
3	5Ru/TiO_2-Plasma	Plasma treated	197
4	5Ru/TiO_2-Conv	Conventional synthesis	157

Table S2. Organosilane oxidation to silanol using TiO_2 supported Ru

No.	Catalyst	Substrate	Conv (%)	Time (min)	Silane/ Ru (TON)	TOF min^{-1}
1	5Ru/TiO_2-Plasma	**1a,** $(CH_3)_2PhSiH$	>99	15	33.3	2.3
2	5Ru/TiO_2-Conv	**1a,** $(CH_3)_2PhSiH$	>99	80	33.3	0.4
3	TiO_2	**1a,** $(CH_3)_2PhSiH$	0	180	100	0
4	None	**1a,** $(CH_3)_2PhSiH$	0	180	100	0

Reaction conditions: Catalyst = 25 mg; Oxidant= 2ml of water; Solvent= 5 ml of Acetone; Temperature=25 °C.

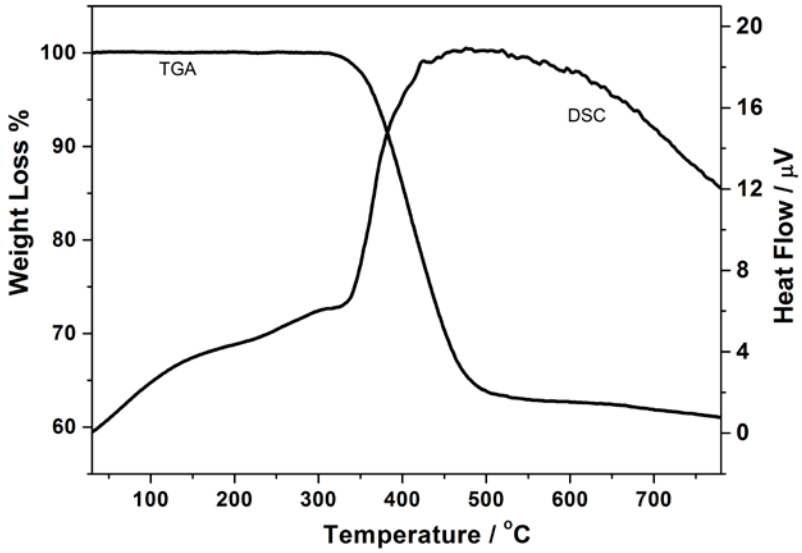

Figure S2. TGA analysis of $RuCl_3$

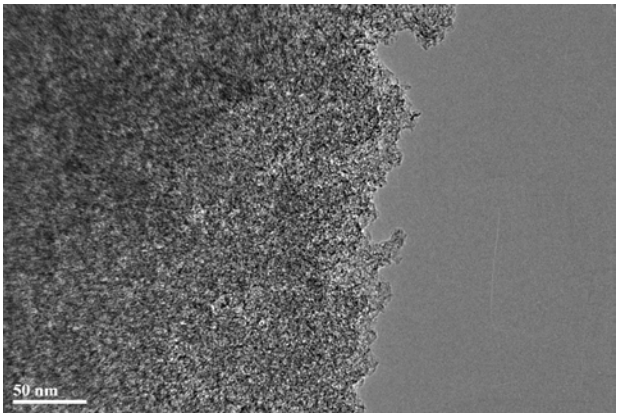

Figure S3. Low resolution TEM image of Ru-Plasma catalyst

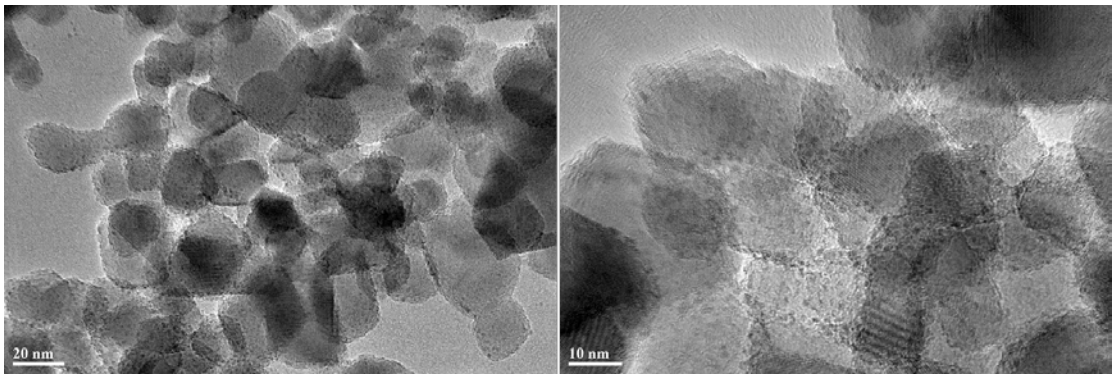

Figure S4. TEM images of Ru/TiO_2 plasma treated sample

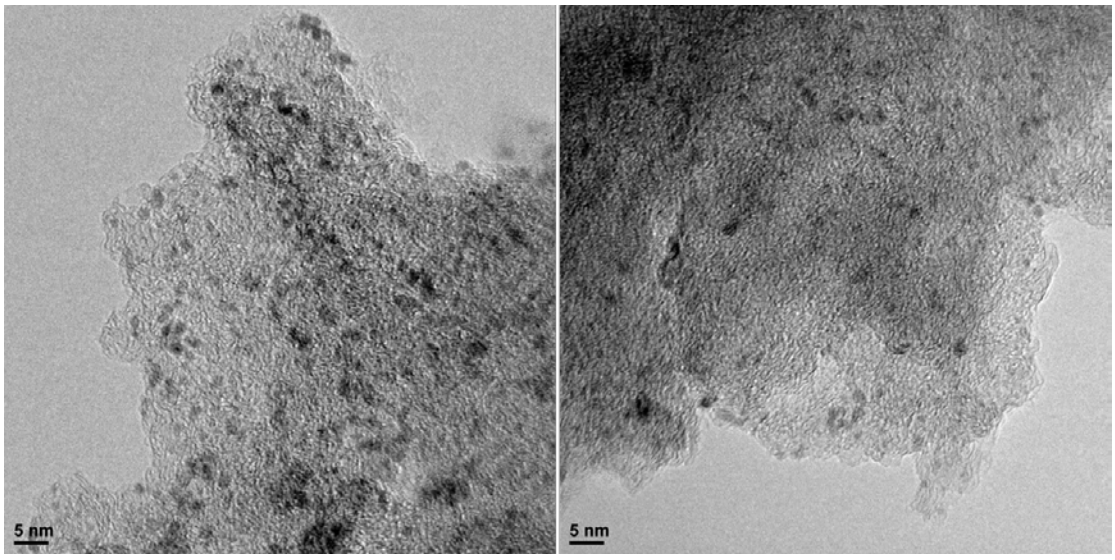

Figure S5. TEM images of Ru-Plasma spent catalyst after three cycles of organosilane oxidation.

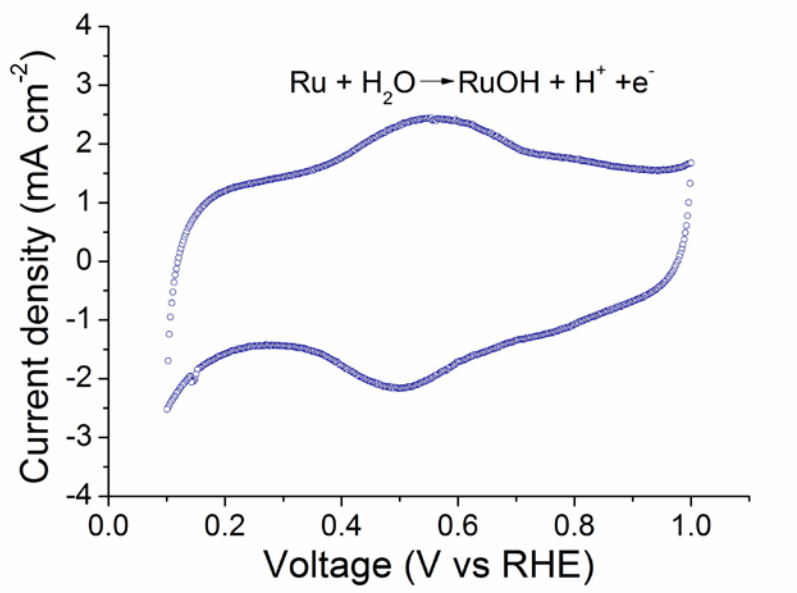

Figure S6. Cyclic voltammetry curve of Ru-Plasma catalyst in 0.05 M deoxygenated H_2SO_4.

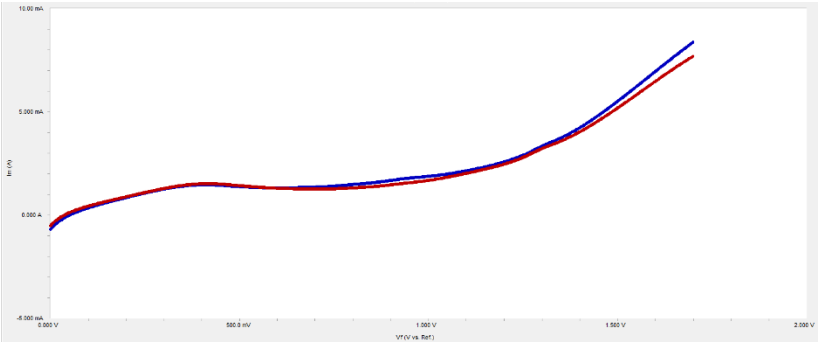

Figure S7. Cycles of LSV for Ru-Plasma to check the reproducibility and stability.

Product Characterization

The product analysis was carried out using a GC (Agilent model 7820A GC system, FID detector, ValcoBond VB capillary column with 30 m length, and 3 µm diameter). ^{1}H NMR and ^{13}C NMR spectra were recorded on a 400 MHz ^{1}H (100 MHz ^{13}C) Bruker AV400 spectrometer in $CDCl_3$. Chemical shifts are reported in ppm (δ) relative to $CDCl_3$ (^{1}H: 7.26 and ^{13}C: 77.36). Coupling constants, *J*, are reported in Hz. Abbreviations are used to express multiplicity: s, singlet; d, doublet; t, triplet; q, quartet; m, multiplet.

Dimethylphenylsilanol, (product from 1a)

^{1}H NMR δ_H(400 MHz; $CDCl_3$) 7.67 – 7.34 (5 H, m, Ph), 2.21 (1 H, br s, OH), 0.41 (3 H, s, CH_3); ^{13}C NMR δ_C(100 MHz; $CDCl_3$) 140.13, 133.33, 129.59, 128.05, 1.22; MS (EI): m/z 152 (M^+, 9%), 137 (100), 77 (3), 75 (3), 45 (6).

Triphenylsilanol (product from 1b)

^{1}H NMR δ_H(400 MHz; $CDCl_3$) 7.87 – 7.12 (15 H, m, Ph), 4.75 (1 H, br s, OH); ^{13}C NMR δ_C(100 MHz; $CDCl_3$) 135.36, 135.31, 130.42, 128.22; MS (EI): m/z 276 (M^+, 58%), 199 (100), 122 (20), 77 (15), 45 (5).

Diphenylmethylsilanol (product from 1c)

^{1}H NMR δ_H(400 MHz; $CDCl_3$) 7.77 – 7.32 (10 H, m, Ph), 3.45 (1 H, br s, OH), 0.71 (3 H, s, CH_3); ^{13}C NMR δ_C(100 MHz; $CDCl_3$) 137.44, 134.29, 130.10, 128.17, 77.36, -0.96; MS (EI): m/z 214 (M^+, 16%), 199 (100), 137 (11), 77 (7), 45 (5).

Triethylsilanol (product from 1e)
^{1}H NMR δ_H(400 MHz; $CDCl_3$) 1.25 (1 H, br s, OH), 0.92 (9 H, t, *J* 8.0, CH_3), 0.51 (6 H, q, *J* 8.0, CH_2); ^{13}C NMR δ_C(100 MHz; $CDCl_3$) 7.17, 6.76; MS (EI): m/z 131 (M^+-H, 75%), 117 (15), 115 (15), 103 (100), 76 (2), 45 (10).

Reference:

1. Madaan, N.; Haufe, R.; Shiju, N. R.; Rothenberg, G., Oxidative Dehydrogenation of n-Butane: Activity and Kinetics Over VO x/Al2O3 Catalysts. *Topics in Catalysis* **2014,** *57* (17-20), 1400-1406.
2. Hernandez-Mejia, C.; Gnanakumar, E. S.; Olivos-Suarez, A.; Gascon, J.; Greer, H. F.; Zhou, W.; Rothenberg, G.; Shiju, N. R., Ru/TiO_2-catalysed hydrogenation of xylose: the role of the crystal structure of the support. *Catalysis Science & Technology* **2015**.
3. Buitrago-Sierra, R.; Jesus Garcia-Fernandez, M.; Mercedes Pastor-Blas, M.; Sepulveda-Escribano, A., Environmentally friendly reduction of a platinum catalyst precursor supported on polypyrrole. *Green Chemistry* **2013,** *15* (7), 1981-1990.
4. Gitis, V.; Beerthuis, R.; Shiju, N. R.; Rothenberg, G., Organosilane oxidation by water catalysed by large gold nanoparticles in a membrane reactor. *Catalysis Science & Technology* **2014,** *4* (7), 2156-2160.